Available online at www.sciencedirect.com
SCIENCE DIRECT®
Journal of Computational and Applied Mathematics 183 (2005) 1–15
JOURNAL OF COMPUTATIONAL AND APPLIED MATHEMATICS
www.elsevier.com/locate/cam

Almost Newton method for large flux steady-state of 1D Poisson–Nernst–Planck equations

Viktoria R.T. Hsu*

University of Utah, Department of Mathematics, 155 South 1400 East, JWB 233, Salt Lake City, UT 84112-0090, USA

Received 21 July 2003; received in revised form 3 December 2004

Abstract

Problems of charge-carrier transport from many different fields converge in mathematics, where they are modeled by a system of Poisson's and Nernst–Planck's equations (PNP) for the electro-static potential and particle dynamics. In this paper, we study a computational steady-state problem of charge-carrier transport. In the case of Dirichlet boundary conditions for the electro-static potential at all locations with given particle densities, the Gummel method (IEEE Trans. Electron Devices 11 (1964) 455) is known to converge to the steady-state solution rapidly, and to high accuracy, so long as the steady-state flux densities remain small. We wish to predict the far from equilibrium, large flux, steady-state of a charged particle system with two compartments, separated by a semi-permeable membrane, in which the electro-static potential is unknown at all but one location with given particle densities. In this case all but one Dirichlet boundary conditions on the electro-static potential are replaced by Neumann boundary conditions. We derive a modified Gummel method (MG) capable of solving such a Dirichlet–Neumann boundary problem. We investigate its difficulties with large steady-state flux densities by comparing it to the full Newton method (FN). Since problems with FN at large steady-state flux densities have been reported (IEEE Trans. Comput. Aid D 7 (2) (1988) 251; J. Appl. Phys. 68 (3) (1990) 1324), we propose, derive, and compare to MG and FN, an almost Newton method (AN) based upon a partial linearization of the problem. AN achieves the same accuracy as MG and FN in only one fifth of the number of iteration steps and retains these qualities even at very large steady-state flux densities.

Keywords: Electrodiffusion; Poisson–Nernst–Planck; Steady-state; Numeric; Iterative; Gummel method

* Tel.: +1 801 581 8340; fax: +1 801 581 4148.
E-mail address: hsu@math.utah.edu (V.R.T. Hsu).

0377-0427/$ - see front matter © 2005 Elsevier B.V. All rights reserved.
doi:10.1016/j.cam.2004.12.024

1. Introduction

Problems of charge-carrier transport have been encountered in many scientific disciplines. To name just a few, in physical devices containing semiconducting materials charges are carried by holes and electrons, and in biological and chemical systems containing semi-permeable membranes charges are carried by ionic species. Charge-carrier transport for these problems converges in mathematics, where they are modeled by a system of Poisson's and Nernst–Planck's equations (PNP). It is common and crucial to study the current–voltage behavior (IV-curve) at steady-state of the considered system based upon an applied potential difference (voltage) between locations of known charge-carrier densities. From the physical point of view this reveals the complete behavior of a device. From the biological point of view it can, for example, give important information about the behavior of ion channels under certain regimes [3,4]. Mathematically, applying a potential difference as described translates to imposing Dirichlet boundary conditions on the electro-static potential when solving for the steady-state of the PNP system.

It has become more important in recent years to study not just how biological systems react to stimuli but understand their behavior in the absence of stimuli by using non-invasive techniques. In this spirit, we wish to predict the steady-state distributions of electro-static potential and particle concentrations in a two-compartment system of charges, in which an internal and an external compartment are separated by a semi-permeable membrane. The membrane is impermeable at its midpoint to larger charged particles, e.g., proteins. The equilibrium of such a system is widely known as the classic Donnan equilibrium. In 1D and a few highly symmetric, higher dimensional cases, the particle distributions and electro-static potential profile at Donnan equilibrium can be obtained analytically for various combinations of valencies in the system. At steady-state, i.e., when particle densities in the bulk are held fixed at values other than their equilibrium values and fluxes are non-zero, no analytic solutions have been found. We therefore seek a method by which to obtain numeric solutions to the steady-state PNP system. Mathematically, and in contrast to *applying* a potential difference, *solving* for it translates to imposing Neumann boundary conditions on the electro-static potential at all but one location of known particle densities. When speaking of Neumann boundary conditions in the remainder of this paper, it is understood that this always involves one normalization condition, such as a Dirichlet condition. The latter is needed since the pure Neumann problem leaves the electro-static potential undetermined up to an additive constant and is thus mathematically not well-posed. However, since any potential is unique only up to an additive constant, the choice of normalization condition is essentially arbitrary.

In contrast to the semiconductor-device equations (SDEs), we consider neither sources of charge-carriers nor fixed space charges (dotation). Sources and sinks of electrons and holes, as considered in the SDEs, correspond to their injection and recombination rates. Employing ionic species as charge-carriers rather than holes and electrons, sources and sinks correspond to chemical reactions in which the species are involved. We do not consider chemical reactions in our setting, and neglect sources and sinks of charge-carriers as taken into account by the SDEs.

We further employ consideration that dynamics in bulk solution are much faster than in the membrane. In the limit of infinitely fast bulk dynamics, particle concentrations and electro-static potential in bulk solution are constant at steady-state, but exhibit a sharp transition from their internal to their external values in a region close to mid-membrane. A more specific, reasonable definition of "close to mid-membrane" has to emerge from the problem parameters defining the width of the membrane, as well as the width of the mathematical boundary layer, at equilibrium. It is reasonable in this setting to focus on the transition layer near mid-membrane, and consider the problem in 1D, which is mathematically modeled by a system

of 1D Poisson's and electrodiffusion equations,

$$\frac{\partial}{\partial x}\left(\varepsilon\frac{\partial\varphi}{\partial x}\right) = -\sum_i z_i c_i, \tag{1}$$

$$\frac{\partial c_i}{\partial t} = \frac{\partial}{\partial x}\left(D_i\frac{\partial c_i}{\partial x} + z_i D_i\frac{\partial\varphi}{\partial x}c_i\right) \equiv -\frac{\partial J_i}{\partial x}, \tag{2}$$

where a subscript i indicates that a quantity is specific to ionic species i, c_i denotes the particle concentration, D_i the diffusion coefficient, z_i the valency, φ the non-dimensional electro-static potential, J_i the flux density and ε a non-dimensional quantity related to the dielectric of the membrane. Our domain of interest is $L \leqslant x \leqslant R$; $L < 0 < R$, and the membrane midpoint lies at $x = 0$.

Boundary conditions (BCs) on the particle concentrations are

$$c_i(L) = c_i^L, \quad \text{and} \quad c_i(R) = c_i^R \quad \text{for all species } i. \tag{3}$$

Assuming net-electroneutrality of the entire two-compartment system, BCs on the electro-static potential in the limit of infinitely fast bulk dynamics are, according to Gauss' Law,

$$\varphi_x(L) = 0 = \varphi_x(R). \tag{4}$$

Considering net-electroneutrality is feasible in our setting even at steady-state, since not meeting it implies the separation of charges by a far distance and is thus energetically not favored. In general, (4) do not define a mathematically well-posed problem because they leave the electro-static potential, φ, undetermined up to an additive constant. We shall revisit this issue in Section (4) when, after discretization, the linearized systems representing some numerical schemes are under-determined and demand an additional normalization condition to be solved successfully. In the remainder of this section, we will derive the flux densities, J_i, and concentration distributions, c_i, as functions of the electro-static potential, φ. From the continuity equation, at steady-state

$$\frac{\partial c_i}{\partial t} = -\frac{\partial J_i}{\partial x} = 0. \tag{5}$$

Therefore the flux density $J_i(x) = J_i = \text{const.}$, and the electrodiffusion equation reduces to Nernst–Planck's equation,

$$-\frac{J_i}{D_i} = \frac{\partial c_i}{\partial x} + z_i\frac{\partial\varphi}{\partial x}c_i, \tag{6}$$

a linear ordinary differential equation for the concentration distributions. Integrating (6) once yields

$$c_i(x)\mathrm{e}^{z_i\varphi(x)} = c_i(x_0)\mathrm{e}^{z_i\varphi(x_0)} - \frac{J_i}{D_i}\int_{x_0}^{x}\mathrm{e}^{z_i\varphi(s)}\,\mathrm{d}s. \tag{7}$$

Continuity of the concentration profiles at mid-membrane of species i permeant to the membrane leads to an expression for the flux density, J_i, of species i,

$$J_i = -D_i\frac{c_i(R)\mathrm{e}^{z_i\varphi(R)} - c_i(L)\mathrm{e}^{z_i\varphi(L)}}{\int_L^R \exp(z_i\varphi(s))\,\mathrm{d}s}, \tag{8}$$

in which the numerator is completely determined by a set of Dirichlet boundary conditions, but not by Neumann boundary conditions, on the electro-static potential. Substituting (8) into (7) eliminates the flux density, and we obtain

$$c_i(x) = \mathrm{e}^{-z_i\varphi(x)} \frac{c_i(L)\mathrm{e}^{z_i\varphi(L)} \int_x^R \mathrm{e}^{z_i\varphi(s)}\,\mathrm{d}s + c_i(R)\mathrm{e}^{z_i\varphi(R)} \int_L^x \mathrm{e}^{z_i\varphi(s)}\,\mathrm{d}s}{\int_L^R \mathrm{e}^{z_i\varphi(s)}\,\mathrm{d}s}, \tag{9}$$

the concentration distribution of the permeant species, i [5]. Species impermeant to the membrane have zero flux density and Boltzmann particle distributions,

$$c_i(x) = \begin{cases} c_i(L)\mathrm{e}^{-z_i(\varphi(x)-\varphi(L))} & \text{for } x < 0, \\ c_i(R)\mathrm{e}^{-z_i(\varphi(x)-\varphi(R))} & \text{for } x > 0. \end{cases} \tag{10}$$

Substituting (9) and (10) into Poisson's equation (1) yields the Poisson–Nernst–Planck (PNP) equation, a highly nonlinear, second order integral–differential equation (IDE) for the electro-static potential, φ,

$$\frac{\partial}{\partial x}\left(\varepsilon\frac{\partial\varphi}{\partial x}(x)\right) = -\sum_i z_i c_i(x, \varphi(x), \mathrm{BCs}). \tag{11}$$

In the remainder of this work, several iterative methods that solve (11) subject to boundary conditions (BCs) (4) are described and compared. In Section 2 the classic Gummel method is introduced, in Section 3 the full linearization of the PNP equation is derived which leads to Newton's method, in Section 4 an almost Newton method based upon a partial linearization is proposed, in Section 5 numeric results are presented, and these are discussed in Section 6.

2. The Gummel method

In this section, we give a brief introduction to the Gummel method [5] as it applies to our setting, i.e., we neglect dotation as well as sources and sinks of charge-carriers as taken into account by the original method.

With the chemical potential, μ_i, of species i, the concentration profile of species i can be expressed as

$$c_i(x) = \mathrm{e}^{\mu_i(x)}\mathrm{e}^{-z_i\varphi(x)}. \tag{12}$$

Substituting (12) into (1) we obtain

$$\frac{\partial}{\partial x}\left(\varepsilon\frac{\partial\varphi}{\partial x}\right) = -\sum_i z_i \mathrm{e}^{\mu_i}\mathrm{e}^{-z_i\varphi}, \tag{13}$$

which is satisfied by the true steady-state electro-static and chemical potentials.

From an initial guess at the electro-static steady-state potential, $\widetilde{\varphi}(x)$, we can compute the corresponding chemical potentials, $\widetilde{\mu}_i(x)$, for each species from comparison of (12) with (9) and (10). We wish to compute a correction, $\delta(x)$, such that $\varphi(x) = \widetilde{\varphi}(x) + \delta(x)$ satisfies Poisson's equation together with the *current* chemical potentials, $\widetilde{\mu}_i$,

$$\frac{\partial}{\partial x}\left[\varepsilon\left(\frac{\partial\widetilde{\varphi}}{\partial x} + \frac{\partial\delta}{\partial x}\right)\right] = -\sum z_i \mathrm{e}^{\widetilde{\mu}_i}\mathrm{e}^{-z_i(\widetilde{\varphi}+\delta)}. \tag{14}$$

Linearization and reorganization yield

$$\frac{\partial}{\partial x}\left(\varepsilon\frac{\partial\delta}{\partial x}\right)-\left(\sum z_i^2 \mathrm{e}^{\widetilde{\mu}_i}\mathrm{e}^{-z_i\widetilde{\varphi}}\right)\delta=-\frac{\partial}{\partial x}\left(\varepsilon\frac{\partial\widetilde{\varphi}}{\partial x}\right)-\sum z_i \mathrm{e}^{\widetilde{\mu}_i}\mathrm{e}^{-z_i\widetilde{\varphi}}, \tag{15}$$

a linear differential equation for δ, which satisfies zero boundary conditions provided the initial guess for the electro-static potential satisfies its Dirichlet boundary conditions. Discretizing (15) by compact finite differences, solving the resulting tri-diagonal system for δ, and taking $\varphi=\widetilde{\varphi}+\delta$ as the next guess at the steady-state potential creates an iterative method, namely the Gummel method [5].

It is a priori not clear whether this method should converge or not. If it does converge, i.e., $\delta\to 0$, then the resulting electro-chemical and electro-static potentials satisfy (13), and we have found the steady-state solution.

The Gummel method was proposed first in 1964 to find the steady-state potential profiles in transistors. In practice, it converges rapidly, at a linear rate, and to high accuracy, so long as the injection and recombination rates of charge-carriers remain small [13]. It has been adapted for higher dimensions, various geometries, many different numerical methods, and has been modified to related numerical schemes. For a mathematical review on the Gummel method and semiconductor modeling, see [10,2]. For an applied review, see [8].

3. Full linearization of the PNP equation

We recognize that in linearizing (13) with respect to the electro-static potential, φ, the dependence of the electro-chemical potentials, μ_i, on φ throughout the domain has been entirely neglected. In this section, we compute the full linearization of (13) for small δ, which takes into account the dependence of the μ_i on φ. We will need to distinguish between trapped and permeant species and introduce the following notation:

$$\alpha_j^x=\sum_{\substack{\text{all } i\\ z_i=j}} c_i(x),\quad \tau_j^x=\sum_{\substack{\text{trapped } i\\ z_i=j}} c_i(x),\quad \tilde{\alpha}_j^x=\alpha_j^x-\tau_j^x. \tag{16}$$

Analogous to (11), substituting (9) and (10) into Poisson's equation (1), yields the Poisson–Nernst–Planck (PNP) equation, the steady-state equivalent of the Poisson–Boltzmann equation

$$\begin{aligned}\frac{\partial}{\partial x}\left(\varepsilon\frac{\partial\varphi}{\partial x}\right)=-\sum_{\text{all}\,j} j\mathrm{e}^{-j\varphi(x)}\Bigg[&\tau_j^L\mathrm{e}^{j\varphi(L)}H(-x)+\tau_j^R\mathrm{e}^{j\varphi(R)}H(x)\\ &+\frac{\tilde{\alpha}_j^L\mathrm{e}^{j\varphi(L)}\int_x^R\mathrm{e}^{j\varphi(s)}\,\mathrm{d}s+\tilde{\alpha}_j^R\mathrm{e}^{j\varphi(R)}\int_L^x\mathrm{e}^{j\varphi(s)}\,\mathrm{d}s}{\int_L^R\mathrm{e}^{j\varphi(s)}\mathrm{d}s}\Bigg],\end{aligned} \tag{17}$$

where H stands for the Heaviside function. We seek a correction, δ, to a guess at the steady-state potential, $\tilde{\varphi}$, such that the true steady-state potential is $\varphi=\tilde{\varphi}+\delta$. In expanding (17) about $\tilde{\varphi}$, we observe that

$$\mathrm{e}^{j(\tilde{\varphi}+\delta)}=\mathrm{e}^{j\tilde{\varphi}}(1+j\delta+\text{h.o.t.}) \tag{18}$$

$$\int_L^x \mathrm{e}^{j(\tilde{\varphi}(s)+\delta(s))}\,\mathrm{d}s=\int_L^x \mathrm{e}^{j\tilde{\varphi}(s)}\mathrm{d}s+j\int_L^x \delta(s)\mathrm{e}^{j\tilde{\varphi}(s)}\,\mathrm{d}s+\text{h.o.t.} \tag{19}$$

$$\frac{1}{\int_L^R \mathrm{e}^{j(\tilde{\varphi}(s)+\delta(s))}\,\mathrm{d}s} = \frac{1}{\int_L^R \mathrm{e}^{j\tilde{\varphi}(s)}\,\mathrm{d}s\left(1+\frac{j\int_L^R \delta(s)\mathrm{e}^{j\tilde{\varphi}(s)}\,\mathrm{d}s}{\int_L^R \mathrm{e}^{j\tilde{\varphi}(s)}\,\mathrm{d}s}+\text{h.o.t.}\right)} \tag{20}$$

$$= \frac{1}{\int_L^R \mathrm{e}^{j\tilde{\varphi}(s)}\,\mathrm{d}s}\left(1-\frac{j\int_L^R \delta(s)\mathrm{e}^{j\tilde{\varphi}(s)}\,\mathrm{d}s}{\int_L^R \mathrm{e}^{j\tilde{\varphi}(s)}\,\mathrm{d}s}+\text{h.o.t.}\right). \tag{21}$$

Substituting into (17) as appropriate, we obtain, after some algebra,

$$\begin{aligned}&\frac{\partial}{\partial x}\left(\varepsilon\left(\frac{\partial\tilde{\varphi}}{\partial x}+\frac{\partial\delta}{\partial x}\right)\right)\\ &\quad=-\sum_{\text{all } j} j\mathrm{e}^{-j\tilde{\varphi}(x)}\Bigg[A_j(x)(1-j\delta(x))+jB_j(x)\delta(L)+jC_j(x)\delta(R)\\ &\qquad+jD_j(x)\int_L^x \delta(s)\mathrm{e}^{j\tilde{\varphi}(s)}\,\mathrm{d}s+jE_j(x)\int_x^R \delta(s)\mathrm{e}^{j\tilde{\varphi}(s)}\,\mathrm{d}s\Bigg],\end{aligned} \tag{22}$$

where

$$A_j(x)=B_j(x)+C_j(x), \tag{23}$$

$$B_j(x)=\mathrm{e}^{j\tilde{\varphi}(L)}\left(\tau_j^L H(-x)+\tilde{\alpha}_j^L\frac{\int_x^R \mathrm{e}^{j\tilde{\varphi}(s)}\,\mathrm{d}s}{\int_L^R \mathrm{e}^{j\tilde{\varphi}(s)}\,\mathrm{d}s}\right), \tag{24}$$

$$C_j(x)=\mathrm{e}^{j\tilde{\varphi}(R)}\left(\tau_j^R H(x)+\tilde{\alpha}_j^R\frac{\int_L^x \mathrm{e}^{j\tilde{\varphi}(s)}\,\mathrm{d}s}{\int_L^R \mathrm{e}^{j\tilde{\varphi}(s)}\,\mathrm{d}s}\right), \tag{25}$$

$$D_j(x)=\frac{\tilde{\alpha}_j^R\mathrm{e}^{j\tilde{\varphi}(R)}-\tilde{\alpha}_j^L\mathrm{e}^{j\tilde{\varphi}(L)}}{\int_L^R \mathrm{e}^{j\tilde{\varphi}(s)}\,\mathrm{d}s}*\frac{\int_x^R \mathrm{e}^{j\tilde{\varphi}(s)}\,\mathrm{d}s}{\int_L^R \mathrm{e}^{j\tilde{\varphi}(s)}\,\mathrm{d}s}, \tag{26}$$

$$E_j(x)=-\frac{\tilde{\alpha}_j^R\mathrm{e}^{j\tilde{\varphi}(R)}-\tilde{\alpha}_j^L\mathrm{e}^{j\tilde{\varphi}(L)}}{\int_L^R \mathrm{e}^{j\tilde{\varphi}(s)}\,\mathrm{d}s}*\frac{\int_L^x \mathrm{e}^{j\tilde{\varphi}(s)}\,\mathrm{d}s}{\int_L^R \mathrm{e}^{j\tilde{\varphi}(s)}\,\mathrm{d}s}. \tag{27}$$

It is easily verified that for $D_j(x)=0=E_j(x)$, and $\delta(L)=0=\delta(R)$, (22) reduces to (15), the equation defining the Gummel method. $\delta(L)=0=\delta(R)$ are the correct boundary conditions for a Dirichlet boundary problem, when the initial guess toward the steady-state potential satisfies its boundary conditions. In the following, the methods used for solving a Neumann instead of a Dirichlet boundary problem are introduced.

4. From modified Gummel to almost Newton method

As a modified Gummel method (MG), we propose an analogous method to the original Gummel method that is capable of solving our Neumann boundary problem. That is, we take into account the corrections to the electro-static potential at the boundaries, and MG is defined by the discretization of (22) with (23)–(25)

and $D_j(x)$ and $E_j(x)$ are replaced by zero. The resulting linear system is sparse, almost tri-diagonal, and therefore efficiently solved. However, both $D_j(x)$ and $E_j(x)$ are proportional to the net flux density of particle species with valency j. If these flux densities become large, the important contributions by the terms containing $D_j(x)$ and $E_j(x)$ are neglected by MG, and we expect it to converge less efficiently.

It is natural to attempt the use of the full Newton iteration (FN) as defined by the discretization of (22) with (23)–(27). However, several problems with FN have been reported: its approach to the steady-state solution can be oscillatory. Not only may these oscillations lead to a low efficiency of this method for relatively small steady-state flux densities, but easily cause overflow for larger steady-state flux densities. Similar problems with Newton's method applied directly to the SDEs have been reported by [11,7], among others, even though its quadratic convergence has been proven by [1] for initial guesses close enough to the solution. Several approaches exist in which transformed or damped variables prevent overflow [2], or small flux densities are neglected [11,12]. Instead of using Newton's method directly, a globally convergent fixed point iteration method, which still incorporates Newton's method, is used by [9,7,6]. In expectation of practical problems with FN we propose an almost Newton method (AN) in the following.

When linearizing the PNP equation (17), we neglect linear corrections due to the denominators, $\int_L^R \mathrm{e}^{j\varphi(s)}\,\mathrm{d}s$. As a result, the equation defining AN is the discretization of (22), where A_j, B_j, and C_j are defined by (23)–(25), but

$$D_j(x) = D_j^* = \frac{\tilde{\alpha}_j^R \mathrm{e}^{j\tilde{\varphi}(R)}}{\int_L^R \mathrm{e}^{j\tilde{\varphi}(s)}\,\mathrm{d}s}, \tag{28}$$

$$E_j(x) = E_j^* = \frac{\tilde{\alpha}_j^L \mathrm{e}^{j\tilde{\varphi}(L)}}{\int_L^R \mathrm{e}^{j\tilde{\varphi}(s)}\,\mathrm{d}s}. \tag{29}$$

In comparison to FN, (28) and (29) define two constants with the same sign, whereas (26) and (27) are obtained by a subtraction of similar terms and likely have opposite signs, thus causing another subtraction of similar terms. In cases in which these terms lead to catastrophic cancellation in FN, we expect to suffer less from this phenomenon when using AN. Further, AN does not neglect flux densities as MG does and thus, in cases in which contributions by flux densities are important, we expect AN to be more robust than MG.

As with the original Gummel method, it is not clear a priori that AN or MG should converge. If they do converge, i.e., $\delta \to 0$, then $\varphi = \tilde{\varphi} + \delta$ is the true steady-state solution we seek. As we shall see, in practice, AN converges rapidly and to the same accuracy as MG or FN, independent of the size of the steady-state flux densities.

4.1. Remarks on the implementation of BCs

Integral to AN, the discretization of (22) with (23)–(25), and (28), (29), is our assumption that for all valencies j, the denominators $\int_L^R \mathrm{e}^{j\varphi(s)}\,\mathrm{d}s$ are not affected by δ, i.e.,

$$\int_L^R \mathrm{e}^{j\tilde{\varphi}(s)}\,\mathrm{d}s = \int_L^R \mathrm{e}^{j(\tilde{\varphi}(s)+\delta(x))}\,\mathrm{d}s \quad \text{for all } j, \text{ or} \tag{30}$$

$$\int_L^R \delta(s)\mathrm{e}^{j\tilde{\varphi}(s)}\,\mathrm{d}s = 0 \quad \text{for all } j \tag{31}$$

in linear approximation for small δ. Obviously, these conditions are dependent on the initial guess of the electro-static potential, and we have as many conditions as there are valencies in the system. AN attempts to meet conditions (31) instead of any normalization condition and, in practice, does an excellent job of doing so. More specifically, the discretization of (22) with (28) and (29) and the Neumann BCs (4) already has full rank. Specifying one's own normalization condition as part of AN results in no convergence. Thus, AN solves the steady-state problem subject to the Neumann BCs (4) without demanding an additional normalization condition for uniqueness reasons. It is easily verified that shifting the electro-static potential by a constant after convergence yields another solution of the PNP equation (17), namely the one satisfying the Dirichlet or normalization condition it was shifted to. To enforce our normalization condition of choice, we therefore simply shift the electro-static potential by an appropriate constant after convergence.

Recall that FN is the discretization of (22) with (23)–(27), and MG is the discretization of (22) with (23)–(25) and $D_j(x)$ and $E_j(x)$ replaced by zero. The linear systems representing FN and MG with BCs (4) are under-determined and each demand one additional condition to be solved for the correction, δ, successfully. Since the resulting electro-static potential, φ, is only unique up to an additive constant, this additional normalization condition is arbitrary. To avoid any bias that may result from choosing, e.g., $\delta(L) = 0$ or $\delta(R) = 0$, instead we choose

$$\int_L^R \delta(x)\,\mathrm{d}x = 0 \tag{32}$$

as additional normalization condition when solving for δ using MG or FN. This choice is natural, too, in the sense that (32) is the linear approximation of (31), the assumption behind AN, for small solutions, φ.

5. Results

We consider a monovalent case, in which the system contains ions of sodium (Na), chloride (Cl), and a large protein (P). The protein carries one negative elementary charge and is confined by the semi-permeable membrane to the left (internal) side of our domain at a concentration of 1 mmol/L. The volume of the internal compartment is four times larger than the volume of the external compartment, and the width of the semi-permeable membrane separating the two compartments corresponds to about 90 Å. To demonstrate individual runs or study the grid refinement of the methods MG, FN and AN we set the internal and external Na concentrations to the physiologically reasonable values of 50 mmol/L and 440 mmol/L, respectively. The resulting net current density is about $-9.75\,\mathrm{mA/cm^2}$. To study the behavior of the methods MG, FN and AN at various steady-states, we hold the internal Na bulk concentration at different values ranging from about 20 mmol/L to 160 mmol/L. This range of internal Na concentrations extends from below the physiologically relevant 50 mmol/L to above the equilibrium value of approximately 140 mmol/L. As a result of keeping the total mass constant in the bulk of the system, the external Na bulk concentration ranges from about 620 mmol/L to 60 mmol/L. The resulting net current densities range from about $-13\,\mathrm{mA/cm^2}$ to $4\,\mathrm{mA/cm^2}$. The asymmetry of this range with respect to vanishing net current at equilibrium results from the chosen range of internal Na concentrations as well as the differing sizes of the two compartments and will be reflected by the results of our steady-state study. For all shown computations, Cl concentrations in the bulk are fixed at values ensuring bulk electroneutrality, and the initial guess toward the electro-static potential is $\varphi(x) = 0$.

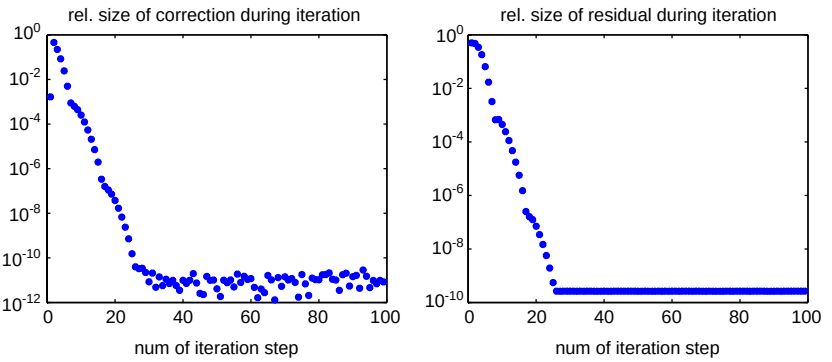

Fig. 1. Left: Maximum absolute value of correction, δ, relative to solution size, φ, versus iteration step. Right: Maximum absolute value of residual, r, relative to local charge, χ, versus iteration step.

5.1. Cutoff criterion

The convergence of all three methods, MG, FN and AN to their maximum accuracy is qualitatively the same. As a typical example, we use FN with $N = 258$ grid points to demonstrate this approach and thus explain the cutoff criterion. Let $A^{(\mathrm{FN})}$ be the linear operator representing FN, let χ denote the discretization of the local charge density, and let D_ε be the linear operator representing

$$\frac{\partial}{\partial x}\left(\varepsilon\frac{\partial}{\partial x}\right),$$

then the residual, r, and the correction, δ, satisfy

$$r = D_\varepsilon\varphi + \chi, \tag{33}$$

$$r = A^{(\mathrm{FN})}\delta. \tag{34}$$

Fig. 1 shows the maximum absolute values of δ relative to φ and of r relative to χ as the iteration proceeds. When the relative size of the correction, δ, reaches its lowest level, the relative size of the residual, r, has already reached its steady, lowest value. Thus, it is sufficient to use only δ in the cutoff criterion. In particular, we demand that δ fall below a certain threshold value. Instead of terminating the iteration at this time, we continue until δ increases for the first time after falling below its threshold and use the solution corresponding to its previous, lower value. Therefore, plotting the maximum absolute value of r relative to χ is not a reproduction of our cutoff criterion but instead documents the lowest relative residual one can expect from any of the considered methods under the given conditions.

5.2. Order of convergence

The order of convergence, $\mathbf{p}$, of each method is described by a power-law for the size of the error in each iteration step. It thus describes how fast the error declines during the iteration. In particular, with δ_k the linear approximation to the error at iteration step k,

$$|\delta_{k+1}| = \mathbf{c}|\delta_k|^{\mathbf{p}} \quad \text{or} \tag{35}$$

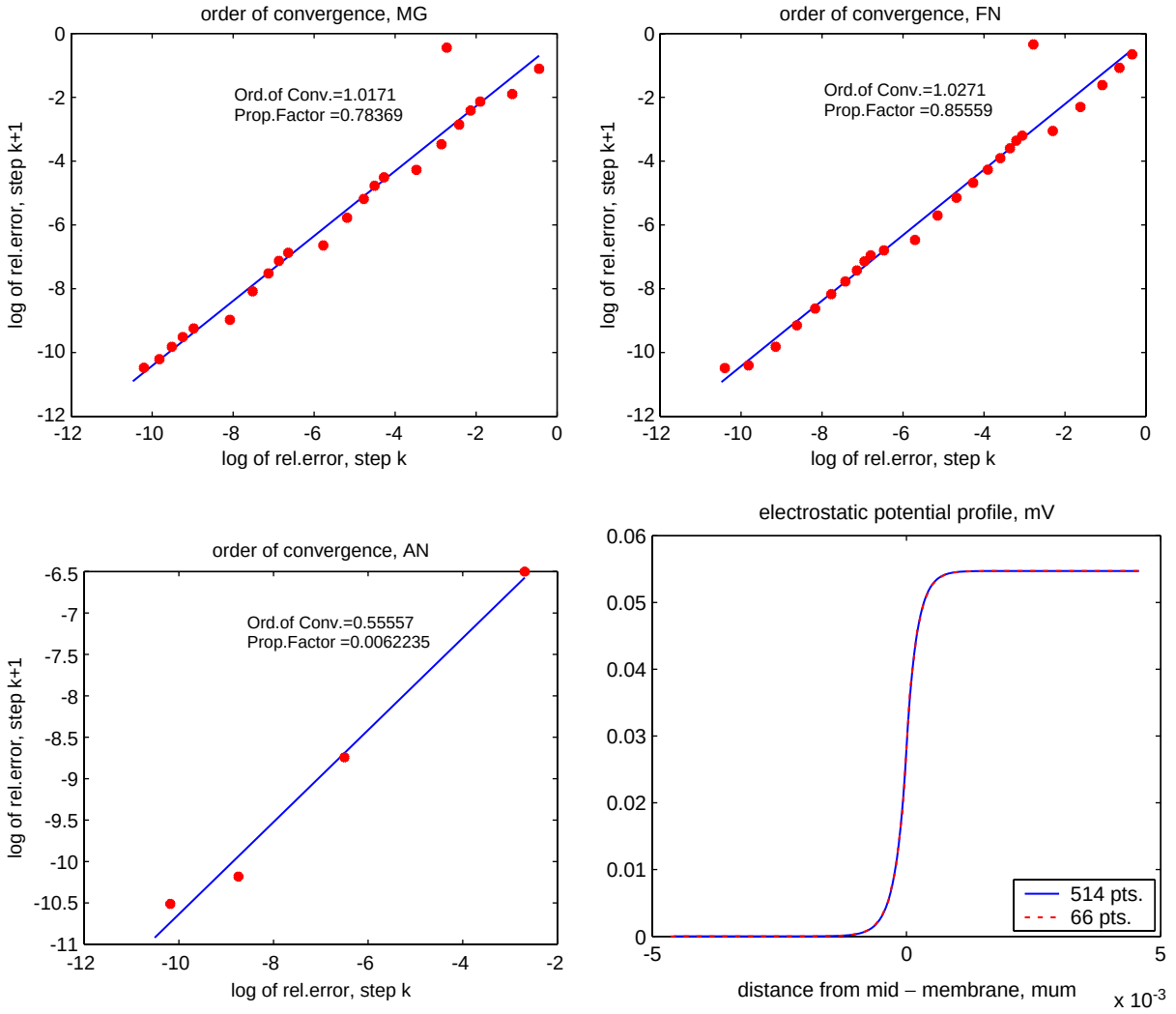

Fig. 2. TL, TR, BL: Order of convergence, **p**, and proportionality factor, **c**, for the approach of MG, FN and AN with $N = 258$ grid points to steady-state. BR: Superimposed profiles of electro-static potential computed with $N = 66$ and $N = 514$ grid points.

$$\log\,|\delta_{k+1}| = \mathbf{p}\,\log|\delta_k| + \log\,\mathbf{c}. \tag{36}$$

The order of convergence is computed from a least-squares fit to (36) throughout this work. Samples of least-squares fits to (36) and the corresponding values of **p** and **c** for MG, FN and AN are shown on the top and lower-left of Fig. 2. The order of convergence of MG is linear, as reported for Gummel's method. It is interesting to note that the overall order of convergence of FN is also linear, even though its quadratic convergence has been proven analytically by [1] for initial guesses close enough to the solution. We speculate that the region around the true solution in which quadratic convergence occurs may be small compared to machine precision, such that, even close to convergence, it has not been entered by the numeric solution of FN. It would be interesting to explore this issue further but this reaches beyond

the scope of this work. AN clearly converges sub-linearly. Despite its sub-linear order of convergence, we shall see that AN may still be more efficient than MG or FN since its proportionality factor, **c**, is of order $O(10^{-3})$ whereas the one of MG and FN is of order $O(10^{-1})$.

5.3. Grid refinement

The superposition of profiles of the electro-static potential computed with a resolution of $N = 66$ and 514 grid points, respectively, are shown on the lower-right of Fig. 2. The two profiles cannot be distinguished by the naked eye, and this demonstrates that profiles of the electro-static potential can be resolved well by using only a few grid points. In the following, results of a grid refinement study are shown that will provide a more systematic understanding of the effect grid refinement has on the results of MG, FN and AN.

The *relative residual* (maximum absolute value of residual, r, relative to local charge, χ) as function of grid resolution is shown on the top-left of Fig. 3. The relative residuals of MG, FN and AN are qualitatively and quantitatively similar and decrease asymptotically to order $O(10^{-10})$. All methods produce relative residuals close to their lowest values from a resolution of about $N = 70$ grid points onward.

The *relative error* in cross-membrane potential (relative deviation from a high-resolution value) as function of grid resolution is superimposed for all methods on the top-right of Fig. 3. It decreases in a log-linear fashion and suggests that, within the tested ranges, below a resolution of about $N = 100$ grid points the cross-membrane potential is accurate to 3 digits, above a resolution of about $N = 100$ grid points 4 digits of accuracy are achieved, and above a resolution of about $N = 700$ grid points one obtains 5 digits of accuracy.

The *number of iterations* until cutoff for MG, FN and AN as function of grid resolution are shown in the middle-left of Fig. 3. The number of iterations taken by all methods does not change much with resolution. MG needs 23 to 26 steps, FN needs 26 to 29 steps and AN needs 4 to 7 steps. Clearly, AN is more efficient than MG or FN by a factor of about 5.

The *net current density* corresponding to the considered steady-state as function of grid resolution is superimposed for all methods in the middle-right of Fig. 3. It approaches its true value asymptotically and reaches values close to its true value from a resolution of about $N = 200$ grid points onward.

The *orders of convergence* of MG, FN and AN as a function of grid resolution are shown on the lower-left of Fig. 3. The computed order of convergence of MG and FN is linear and does not change much for different grid resolutions. The computed order of convergence of AN is clearly sub-linear and varies from 0.55 to 0.8.

The *order of accuracy* of each method relates the true solution, φ_{true}, its discrete approximation, φ_N, and the grid resolution of the discrete solution of N points by a power-law. It thus describes how the accuracy of the discrete solution improves with increasing resolution and may take the form

$$\varphi_{\text{true}} = \varphi_N + \mathbf{a}N^{-\mathbf{q}}. \tag{37}$$

The order of accuracy, **q**, of φ_N may be estimated from three discrete solutions with consecutively doubling resolutions as

$$\mathbf{q} = \log\left(\frac{|\varphi_{2N} - \varphi_{4N}|}{|\varphi_N - \varphi_{2N}|}\right) \Big/ \log\left(\frac{1}{2}\right). \tag{38}$$

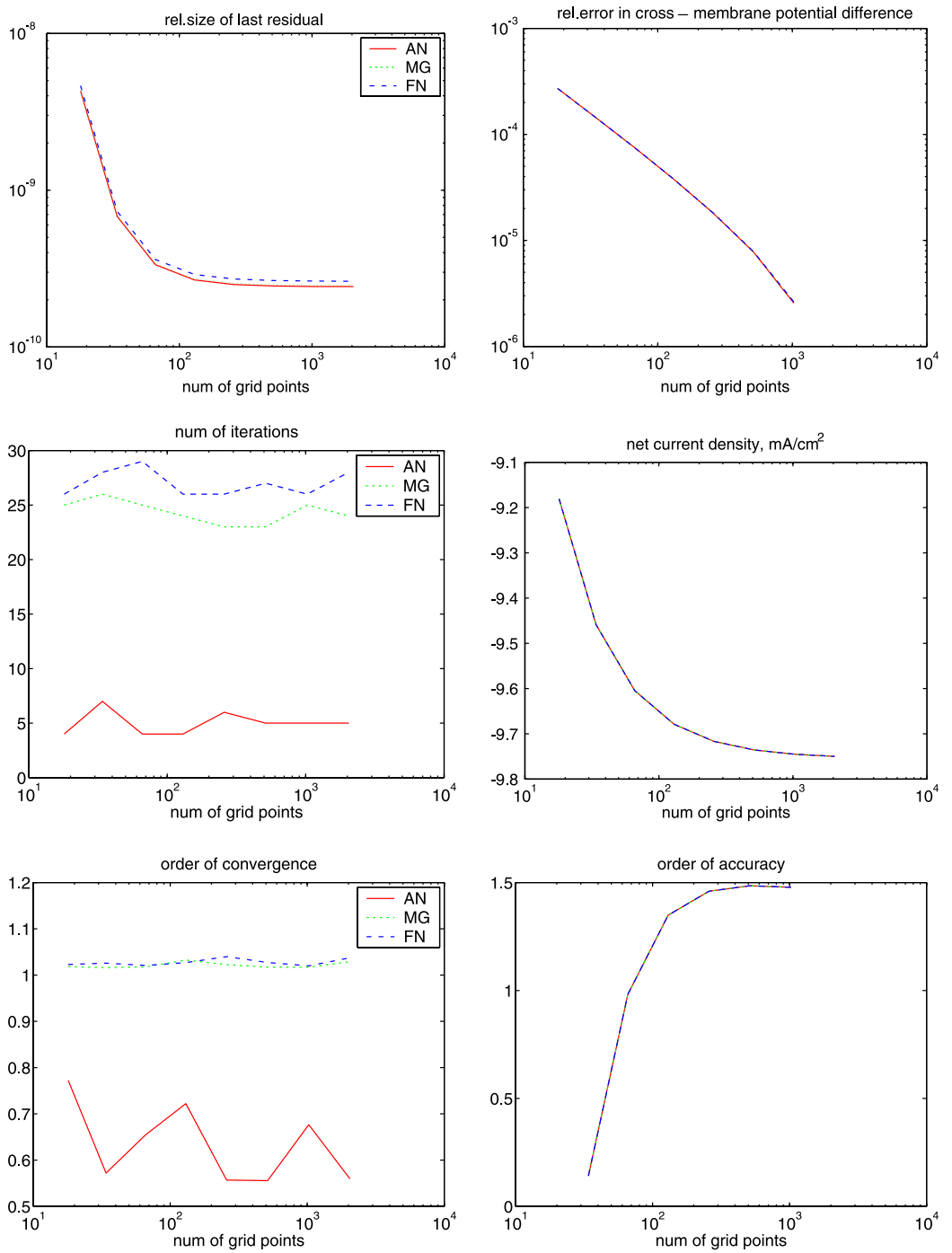

Fig. 3. Results at one steady-state for various grid resolutions. TL: Maximum absolute value of residual, r, relative to local charge, χ. TR: Relative deviation of cross-membrane potential from the value computed with $N = 2050$ grid points, superimposed for MG, FN and AN. ML: Number of iterations taken by MG, FN and AN. MR: Net current density of the considered steady-state, superimposed for MG, FN and AN. BL: Order of convergence of MG, FN and AN. BR: Order of accuracy, superimposed for MG, FN and AN.

The orders of accuracy of MG, FN and AN are superimposed in the lower-right of Fig. 3. The order of accuracy asymptotically approaches 1.5. It equals approximately unity for a resolution of $N = 70$ grid points and reaches values close to 1.5 at resolutions about above $N = 200$ grid points.

5.4. Steady-state study

The *number of iterations* until cutoff for MG, FN and AN for various steady-states are shown on the top-left of Fig. 4. The number of iterations taken by AN at various steady-states does not change much, ranges mostly from 4 to 8 steps and reaches at most 15 steps. The number of iteration steps taken by MG and FN at various steady-states is lowest near equilibrium, when the net current density vanishes. Near equilibrium, MG and FN take about 5 to 10 steps to cutoff, similar to AN. At steady-states farther away from equilibrium, the iteration steps needed by MG and FN rapidly increase to about 25 and 30 steps, respectively. The advantage of AN is not only that it is faster than MG and FN but also that its convergence is independent of the size of the net current density.

The *relative residuals* of MG, FN and AN for various steady-states are superimposed on the top-right of Fig. 4. All methods produce qualitatively and quantitatively similar results. In particular, the relative residual is smallest in the immediate vicinity of the equilibrium, rapidly increases near equilibrium and appears to linearly increase and decrease toward positive and negative net current densities, respectively.

The *orders of convergence* of MG, FN and AN for various steady-states are shown on the lower-left of Fig. 4. The computed order of convergence of MG and FN is linear and does not change much between different steady-states. The computed order of convergence of AN is clearly sub-linear and varies quite unpredictably from 0.55 to 0.9. We believe that part of the reason for this variation lies in the fact that, because of its fast convergence, the order of convergence of AN results from a least-squares fit to only a few points. Thus, for only one or two iteration steps more or less the relative change in the number of points contributing to the least-squares fit is large, causing a large variation in the slope of the least-squares line. This hypothesis is supported by the increased variation in the order of convergence of MG and FN near equilibrium, where both methods require many fewer iteration steps to cutoff.

The *current–voltage relationship* (*IV* -curve) for the considered steady-states is superimposed for MG, FN and AN for various steady-states on the lower-right of Fig. 4. All three methods produce the same *IV*-curve.

6. Discussion

We have given a brief introduction to the original Gummel method [5] for solving the steady-state PNP equations subject to a set of Dirichlet boundary conditions. We have derived a modified Gummel method (MG) as the easiest adaptation of the Gummel method for solving the steady-state PNP equations as a Neumann boundary value problem. We have computed the full linearization of the PNP equation, the discretization of which, (22) defines the corresponding full Newton iteration (FN). The full linearization of the PNP equation has revealed that the same nonlinear coefficients that are proportional to flux densities and may lead to catastrophic cancellation in FN, as reported in literature (compare Section 4), are completely neglected by MG. Thus MG's remaining sensitivity to flux densities has been explained by its neglect of terms proportional to flux densities.

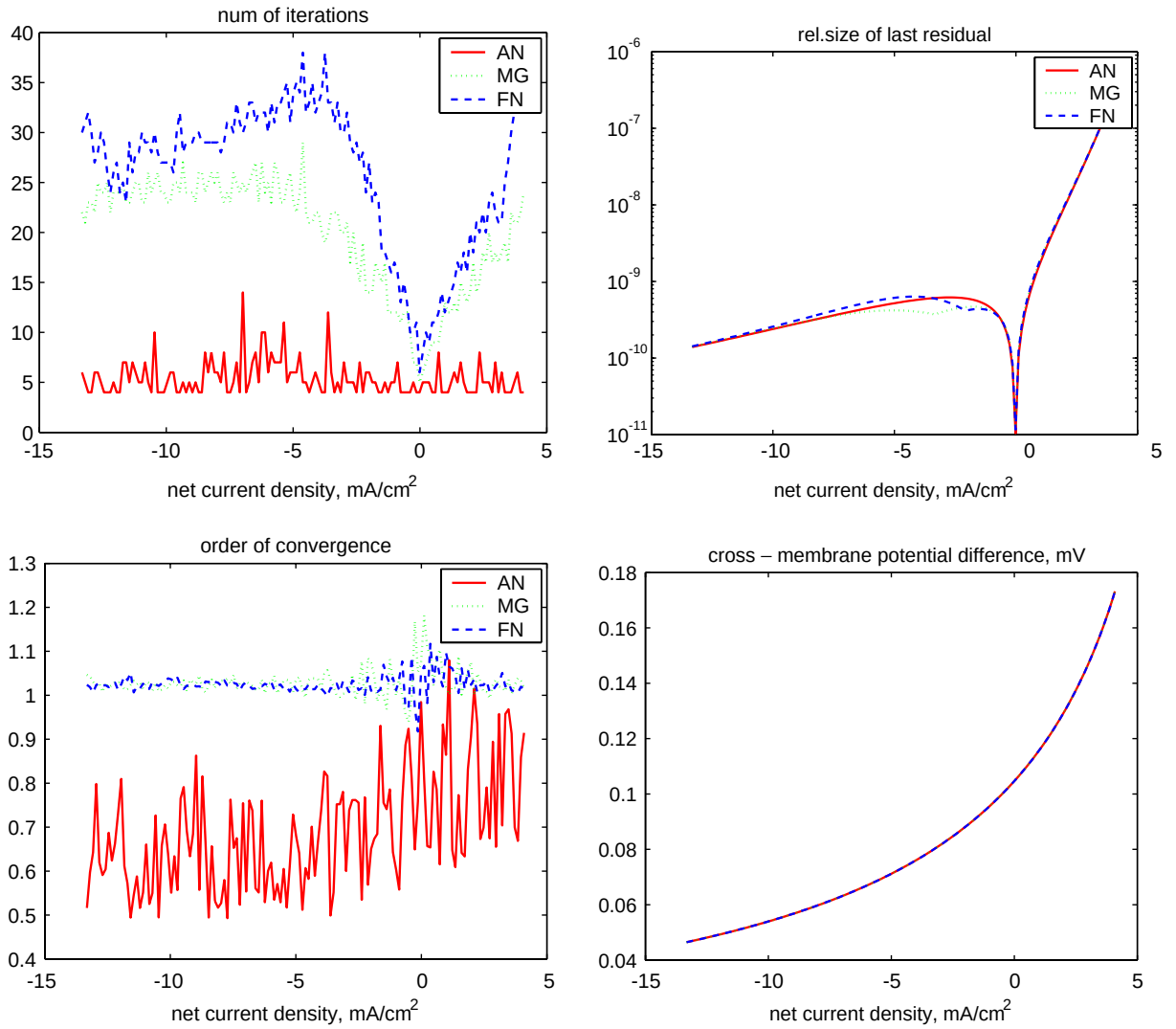

Fig. 4. Results for various steady-states computed at a resolution of $N = 258$ grid points. TL: Number of iterations taken until cutoff by MG, FN and AN. TR: Maximum absolute value of residual, r, relative to local charge, χ. BL: Order of convergence of MG, FN and AN. BR: Current–voltage relationship (IV -curve).

We have derived an almost Newton method (AN) for solving the PNP equation as a Neumann boundary value problem by neglecting the denominators in the linearization of the PNP equation. AN, as well as FN, is represented by a dense linear system and requires a high effort to obtain the solution at each iteration step compared to MG. However, AN has been shown to avoid FN's problems with catastrophic cancellation as well as MG's sensitivity to flux densities that stems from neglecting them. AN converges with about one fifth of the number of iteration steps to the same accuracy as MG and FN and is insensitive to changes in flux densities. AN also converges faster than MG and FN in absolute time which implies that it needs fewer flops. Therefore, AN is an excellent candidate for the simulation of consecutive steady-

state dynamics between the two bulk compartments of the system. For such simulations it is required to compute the solution to many steady-state problems and is desired to do so efficiently.

In future work we would like to apply AN to simulating dynamics via a consecutive steady-state approximation in two-compartment systems as considered in this paper. We are especially interested in physiologically realistic bulk concentrations which, in this work, have resulted in net current densities of about $-10\,\mathrm{mA/cm^2}$. We would also like to modify AN to solving a different steady-state problem, in which the trapped, large particles cannot enter the semi-permeable membrane, thus resulting in two double layers at each membrane–bulk interface. This would require one to extend the computational domain beyond the membrane region and to consider piecewise constant diffusion coefficients and dielectrics. Preliminary computations suggest that the convergence of MG, FN and AN is much slower in this setting. We would further like to extend AN to solving the biochemical equivalent of the semiconductor-device equations (SDEs) in the presence of recombination currents and dotation. That is, we wish to extend AN to solving the 1D, steady-state PNP equations in the presence of chemical reactions, as well as charges inherent to the semi-permeable membrane.

Acknowledgements

I thank B. Eisenberg for pointing me toward Gummel's method, H. Qian and A. Fogelson for helpful discussions, and H. Qian, M. Kot, B. Guy and A. Fogelson for reviewing the manuscript.

References

[1] P. Amster, R. Pinnau, Convergent iterative schemes for a non-isentropic hydrodynamic model for semiconductors, Z. Angew. Math. Mech. 82 (8) (2002) 559–566.
[2] K.H. Bach, H.K. Dirks, B. Meinerzhagen, et al., A new nonlinear relaxation scheme for solving semiconductor-device equations, IEEE Trans. Comput. Aid D 10 (9) (1991) 1175–1186.
[3] B. Eisenberg, Ionic channels in biological membranes—electrostatic analysis of a natural nanotube, Contemp. Phys. 39 (6) (1998) 447–466.
[4] R.S. Eisenberg, From structure to function in open ionic channels, J. Membrane Biol. 171 (1) (1999) 1–24.
[5] H.K. Gummel, A self-consistent iterative scheme for one-dimensional steady state transistor calculations, IEEE Trans. Electron Devices 11 (1964) 455–465.
[6] D.C. Kerr, I.D. Mayergoyz, 3-D device simulation using intelligent solution method, VLSI DES 6 (1–4) (1998) 267–272.
[7] C.E. Korman, I.D. Mayergoyz, A globally convergent algorithm for the solution of the steady-state semiconductor-device equations, J. Appl. Phys. 68 (3) (1990) 1324–1334.
[8] H. Kosina, E. Langer, S. Selberherr, Device modeling for the 1990s, Microelectron. J. 26 (2–3) (1995) 217–233.
[9] I.D. Mayergoyz, Solution of the nonlinear Poisson equation of semiconductor-device theory, J. Appl. Phys. 59 (1) (1986) 195–199.
[10] R. Pinnau, A review on the quantum drift diffusion model, Transport Theor. Stat. 31 (4–6) (2002) 367–395.
[11] C. Ringhofer, C. Schmeiser, A modified Gummel method for the basic semiconductor-device equations, IEEE Trans. Comput. Aid D 7 (2) (1988) 251–253.
[12] C. Ringhofer, C. Schmeiser, An approximate Newton method for the solution of the basic semiconductor-device equations, SIAM J. Numer. Anal. 26 (3) (1989) 507–516.
[13] S. Selberherr, Analysis and Simulation of Semiconductor Devices, Springer, Berlin, 1984.